Advances in Aircraft and Spacecraft Science, *Vol. 8, No. 3 (2021) 239-250*
https://doi.org/10.12989/aas.2021.8.3.239

An investigation of boat-tail helmet to reduce drag

Khizar A. Pathan*[1], Sher A. Khan[2a], Aadil N. Shaikh[1], Arsalan A. Pathan[1] and Shahnawaz A. Khan[3]

[1]Department of Mechanical Engineering,
Trinity College of Engineering and Research, Pune, Maharashtra, 411048, India
[2]Department of Mechanical Engineering, Faculty of Engineering,
International Islamic University Malaysia, Kuala Lumpur, Selangor, Malaysia
[3]Oil and Gas Division, Siemens Energy, Pune, Maharashtra, 411013, India

(Received May 18, 2021, Revised August 6, 2021, Accepted August 25, 2021)

Abstract. A helmet is a kind of shielding equipment used to shield the head from fatal injuries. The helmet experiences drag while moving at a certain velocity. The total drag on the helmet increases with an increase in velocity. The drag force at high velocity has a significant effect on the rider's neck and may result in cervical spondylosis. Now a day's neck pain, neck sprain, spondylosis have become significant issues related to the human body. The reduction of drag on the helmet will be a boon for society, which will reduce the force on the neck. The decrease in drag is an essential field of study. The drag force can be reduced by various methods like coating on the surface, modifying the helmet's shape, etc. The study's purpose is to decrease drag on the helmet by improving the helmet's shape. The CFD analysis is carried out to find the best profile of the helmet and fineness ratio of the boat-tailed helmet to minimize drag. The CFD results are validated with the wind tunnel laboratory outcomes. Based on the findings, a considerable reduction in the drag is accomplished at the velocity of 32.5 m/s.

Keywords: boat-tail; CFD; drag; helmet

1. Introduction

The helmet covered the head protected it from injury in case of accidents. The helmet helps the head in shielding the human head. In civilian development, helmets are utilized for recreational pursuits and plays, critical activities, and transportation. Since the 1990s, most helmets are created of resin or plastic materials. The vital aspect is the much feasible head security in a collision. The helmet should guard not just against free injuries but also notable acceleration-deceleration. Helmet durability even a helmet strength to fast absorb energy should be guided by effective helmet aerodynamics. The resulting drag should be as tiny as possible to produce a decreased influence on the human body, particularly the neck. The different forces acting on a helmet are skin friction drag, base drag, and wave drag. The drag can be reduced by giving streamline shape to the moving body. The coefficient of drag for various shapes is given in Table 1 V. C. Sathish Gandhi *et al.* (2014). The drag coefficient is generally depending on shape of the object and the

*Corresponding author, Associate Professor, E-mail: kn.pathan@gmail.com
[a]Professor, E-mail: sakhan@iium.edu.my

http://www.techno-press.org/?journal=aas&subpage=7 ISSN: 2287-528X (Print), 2287-5271 (Online)

Reynolds number. Based on the basics of aerodynamics it is cleared that the to get minimum drag the shape of the moving body should be in streamline.

Drag can be overcome by improving the helmet shape, i.e., decreasing the drag coefficient. Today's manufacturing technologies allow us to manufacture highly advanced shapes. Typical production processes involve material lamination or thermoplastic processing. A rounded shape enhances not just helmet aerodynamics but also helmet strength. One approach to aerodynamically investigate the motorcycle helmet is a CFD analysis that allows the distribution of velocity and pressure on the exterior and throughout the investigation. The CFD analysis is verified by laboratory experiments on the model.

Khan S.A. *et al.* (2019a) investigated the various types of submarines used in events like ISR and eISR are analyzed and found the optimum fineness ratios for different shapes. The multiple shapes of submarines like Conic shape hull, Elliptical shape hull are used for the CFD analysis by flowing water at velocities of 3, 4, and 5 m/s. The fineness ratios at which the drag is minimum are found in submarine shapes of the study. Beaumount *et al.* (2018) referred the study of the streamline models and explained that the airflow trajectories about the cyclist depend on the shape of the helmet and the head's position. It was determined that the boundary layer and the entire airflow behavior were changed. The existing studies (Pathan *et al.* 2019, 2020; Quadros *et al.* 2020) are available in the literature on passive control methods to reduce drag. Shaikh *et al.* (2020) have studied the flow through the catalytic converter to minimize pressure drop by varying the inlet cone angles. Abdul Abid *et al.* (2021) has studied unmanned aerial vehicle wing profile using CFD analysis and found that the results shows better flow visualization at low Reynolds numbers.

Mehta (2020) have worked on forward facing aerospike numerically and experimentally and found that the drag can be reduced by forward facing aerospike up to 36.47% at Mach number 2.0. He has studied various cases with aerospike and without aerospike for transonic and low supersonic Mach numbers and found that the drag can be reduced in the range of 18.1 to 36.47 for Mach numbers 0.8 to 2.0. R. Kalimuthu *et al.* (2019) have studied performance of spikes on blunt body at Mach number 6. Beaumont *et al.*(2018) has used computational fluid dynamics to study aerodynamic analysis of helmet by varying head positions and found that cyclist significantly influences the performance by varying the head position. Brownlie *et al.* (2010) worked experimentally in wind tunnel on cycling helmets by varying yaw angle 0 to 15^0. Alam *et al.* (2014) have experimentally studied four models of helmets, two having smooth surface and two having ribbed surface, to understand the effectiveness of ribs on the performance of helmet. They found that there is no measurable advantage of ribs on the helmet performance. Paul M. *et al.* (2018) studied experimentally in wind tunnel athletes riding posture and found frame clench setup as most aerodynamic tandem setup. Meng *et al.* (2021) have performed fluid thermal coupling analysis of flying vehicles at high speeds and concluded that the drag value and heating level related to reattachments shock and angle.

Further, the drag force on the helmet can be reduced by decreasing the helmet viz's the frontal area by modifying the helmets dimensions as providing a significantly less frontal area. Due to the drag, people feel a significant amount of resistance while driving motorbikes and cycle. Due to this, some people may discover acute pain in their necks, and also some may face diseases like Spondilysis at a very young age and hence may face discomfort in wearing the helmet. To better the society and the objective of letting the racers win by some milliseconds in the race, and it is of utmost importance to reduce the drag acting on the helmet and make the helmet more aerodynamically stable and with minimum possible.

Several helmet manufacturers have recently introduced various helmet materials, and several

helmet manufacturers have introduced various helmet materials to strengthen and reduce skin friction drag. Alam *et al.* (2014) referred to reduce further the helmet's aerodynamic drag; the helmet manufacturers have worked on various shapes and sizes of the helmet. Though, no separately verifiable study so far has been published on the aerodynamic review of the boat-tailed helmet. Hence, the investigation's main aim was to observe the effect of the fineness ratio of the boat tail helmet using CFD analysis and to validate the results by experimentation.

A boat tail is a streamlined body having a shape similar to that of bullets or rockets used in military cavalry. The boat tail is also called a sealed undercover body, whose concept was used in the late '90s. In the present research work, helmet's modification is to attach the boat tail on the helmet rear portion to reduce base drag. Such a significant difference in drag causes a crucial win for the biker, cyclist, or racer when participating in a professional race.

In the literature no one has worked on the boat tail helmet to reduce drag. In this research work a cone called boat tail is attached with the helmet to reduce drag.

2. Modelıng and meshıng and cfd analysıs

2.1 Modeling

The parameters of the study are the length and diameter of the cone (boat tail), which is attached to the rear side of the helmet. Fig. 1 shows the parameters, i.e., length (L) and diameter (D) of the cone. The length of the cone is the axial height of the cone, and the diameter is the base diameter of the cone. The cone diameter is equal to the diameter of the hemisphere of the helmet.

The helmet geometries are modeled with four fineness ratios (length to base diameter ratios of cone) 1.0, 1.5, 2.0, and 2.5 to find best fineness ratio, which gives minimum drag. The conical boat tail was attached at the rear end of the helmet. The length of the boat tail of the helmet was varied by keeping the boat tail constant's cone diameter.

In the modeling, the helmet's cone diameter was kept constant at 220 mm, and lengths of boat tail were varied by controlling the cone length to diameter ratios 1.0, 1.5, 2.0, and 2.5. The boat tails' calculated sizes for L/D ratios 1.0, 1.5, 2.0, and 2.5 are 220, 330, 440, and 550 mm, respectively.

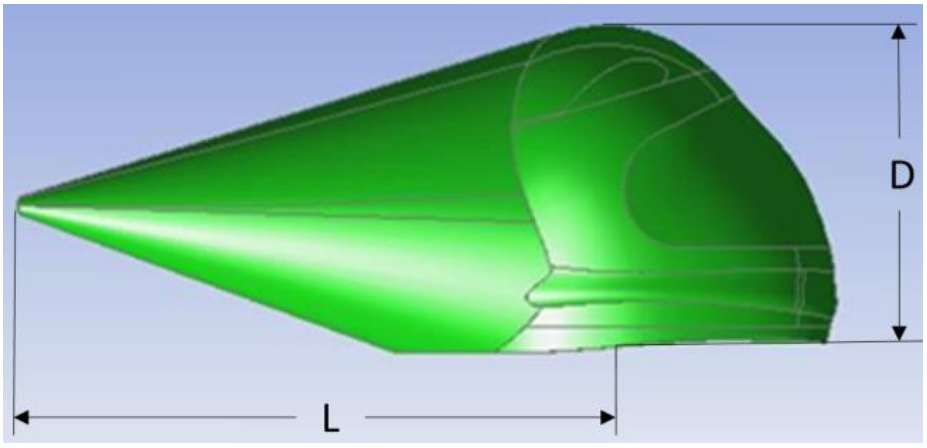

Fig. 1 Parameters of boat tail helmet

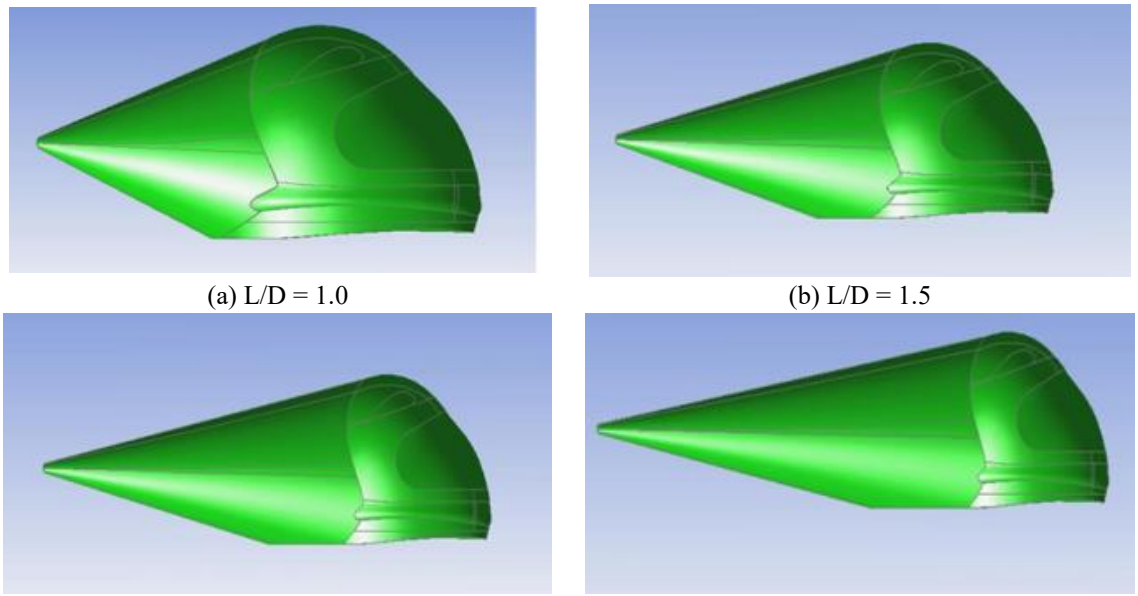

(a) L/D = 1.0 (b) L/D = 1.5

(c) L/D = 2.0 (d) L/D = 2.5

Fig. 2 Boat-tailed helmet with various cone length to diameter ratios

Table 2 Details of mesh size and number of mesh elements for grid independence test

Sr. No.	Mesh Element Size (mm)	No. of Mesh Nodes	No. of Mesh Elements
1	130	31531	40401
2	120	32239	40566
3	110	34747	42960
4	100	39229	48190
5	90	43827	52339
6	80	50111	58184
7	70	62723	71695
8	60	82792	92053
9	50	119377	129051
10	40	197978	209009
11	30	408489	424536
12	20	1264983	1305857
13	10	8618407	9007058

Figs. 2(a), 2(b), 2(c) and 2(d) show the helmet models with cone length to diameter ratios 1, 1.5, 2.0, and 2.5, respectively.

The box-type enclosure considered for the CFD analysis was five times the dimensions of the helmet in X, Y, and Z directions.

2.2 Meshing

Proper meshing is an essential task for getting accurate results because if the meshing is not

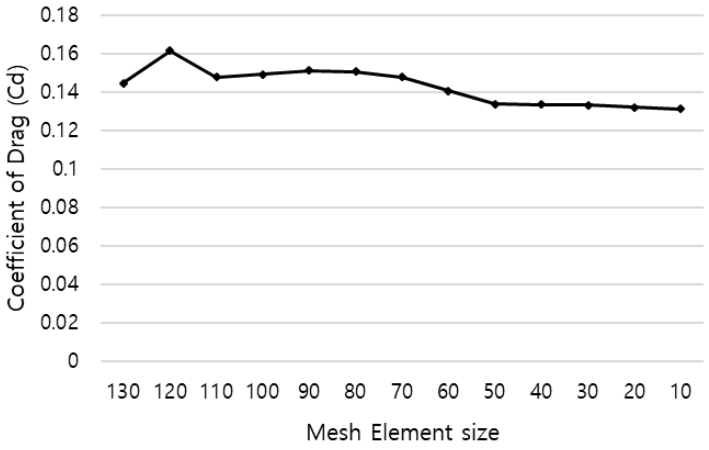

Fig. 3 Grid independence test: Mesh element size Vs Coefficient of drag

correct, it will lead to errors in CFD results. The choice of the element type depends on the complexity of the geometry and the computational resources available. Usually, the hexahedral meshes for simple geometries are used; unstructured tetrahedral meshes with prism layers for complex geometries and pure tetrahedral meshes for too complex geometries. Here, in this case, we used Hex Dominant mesh, and the mesh's quality is superior.

The grid independence test is an important test to find the effectiveness of grid size on results. The accuracy of results and the time required for simulation are depends on the size of grid. To optimize the time required for simulation is the grid independence test plays an important role. Before proceeding to the actual work, the grid independence test is performed. Table 2 shows the details of mesh size and corresponding number of mesh elements.

The results of coefficient of drag is extracted from the software and plotted. Fig. 3 shows the results of drag coefficient for various grid sizes. From the results it is clear that if the mesh element size is reduced to 50 or less the change in the results is negligible. Based on the results the mesh element size of 50 mm is considered for further analysis work.

2.3 CFD analysis

Based on the boundary condition the Reynold number calculated as 1.4×10^6. The k-epsilon turbulent model is selected for the analysis. The k-epsilon turbulent model gives best results over a wide range on analysis (Khan *et al.* 2019a, Pathan *et al.* 2019,2020). Boundary conditions are defined at the inlet as velocity inlet and outlet as pressure outlet. After setting the required boundary conditions solution is initialized and at least 10000 iterations are carried out using viscous - standard k-epsilon, the standard wall function model. The solution seemed to be converged in many cases within 500 iterations. At the end of the solver iteration, the residual sum for each conserved variables is computed and stored.

Realizable k-epsilon scalable wall function turbulence model is used with boundary conditions and model constants Epsilon 1.9, TKE Prandtl number 1, TDR Prandtl number 1.2, Energy Prandtl number 0.85 and wall Prandtl number 0.85.

The pressure velocity coupling solution algorithm is used. COUPLED Pressure Velocity Coupling Scheme is used for the analysis. In the spatial discretization the setting used are gradient:

least square cell based, pressure: second order, momentum: second order upwind, turbulent kinetic energy: first order upwind, turbulence dissipation rate: first order upwind and energy: second order upwind. If the velocity field is known, then the standard Euler equation is given in Eq. (1).

$$\left[\frac{\partial \rho u}{\partial x}+\frac{\partial \rho v}{\partial y}+\frac{\partial \rho w}{\partial z}\right]=0 \tag{1}$$

After substituting the value of Φ with standard direction vector of velocity u, v and w, the momentum equations are given in Eqs. (2) and (3).

$$\left[\frac{\partial \rho u u}{\partial x}+\frac{\partial \rho v u}{\partial y}=\frac{\partial \frac{v \partial u}{\partial x}}{\partial x}+\frac{\partial \frac{v \partial u}{\partial y}}{\partial y}-\frac{\partial p}{\partial x}+S_u\right] \tag{2}$$

$$\left[\frac{\partial \rho u v}{\partial x}+\frac{\partial \rho v v}{\partial y}=\frac{\partial \frac{v \partial v}{\partial x}}{\partial x}+\frac{\partial \frac{v \partial u}{\partial y}}{\partial y}-\frac{\partial p}{\partial y}+S_v\right] \tag{3}$$

where u, v, are the x- and y-directional components of velocity, ρ is the density, $S_{u,v}$ are the source terms, and p is the pressure field.

2.4 Results

The results were plotted after the solutions were converged. Different parameters were verified for calculations and experimentation purposes. Fig. 4(a) show that the pressure is high at the frontal area of the helmet as it is the first portion that comes in contact with air and responsible for maximum drag. But due to the addition of the boat tail at the rear end side of the helmet, the pressure over the boat tail is uniformly distributed. Hence reduces the base drag of the helmet. This causes a drastic reduction in the drag on the helmet, providing a better sense of comfort and beneficial from the aerodynamic point of view. Fig. 4(b) shows the turbulence intensity in percentage.

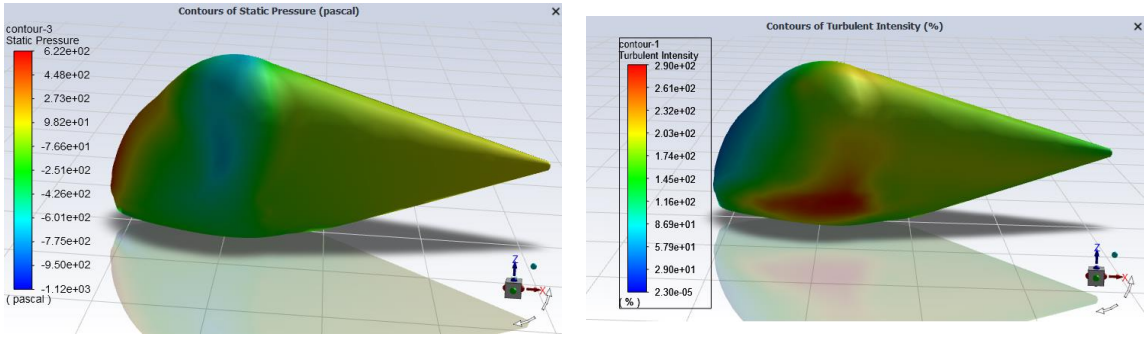

(a) Contour of static pressure (Pa) (b) Contour of turbulence intensity (%)

Fig. 4 Contours of static pressure and turbulence intensity on the helmet with L/D = 1.5 at 32.5 m/s

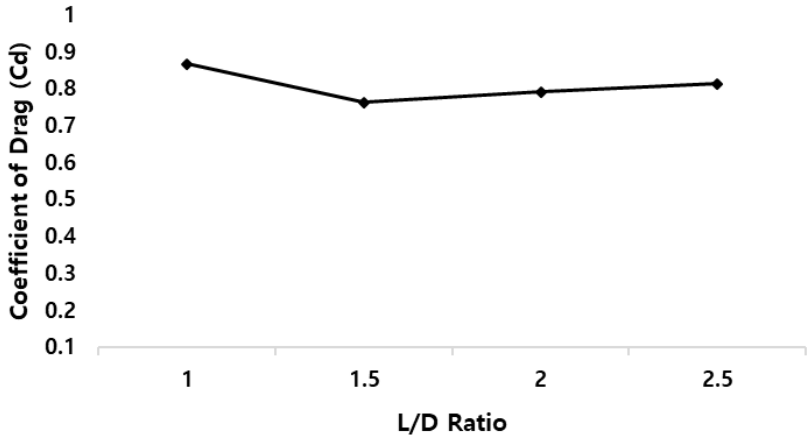

Fig. 5 Coefficient of drag (Cd) for various L/D ratios at 32.5 m/s

All the models with different L/D ratios were analyzed in ANSYS Workbench and Fluent. The calculations were noted and plotted to compare the results of other models. It was observed that attaching the boat tail to the helmet significantly reduces the drag acting on the helmet.

The results of drag force are recorded and base on the results, the coefficient of drag is calculated using Eq. (4).

$$C_D = \left[\frac{2F_d}{\rho A V^2} \right] \tag{4}$$

where,
F_d is drag force
ρ is density of air
A is projected area of helmet
V is velocity

All the results were plotted on a chart for the ease of understanding, which is shown in Fig. 5. The graph shows a decrease in drag in the first instance. Still, it further rises, which makes us sure to consider an exact length for the boat tail of helmet, making us sure to consider an exact length for the helmet for further experimentation of the helmet in the wind tunnel. An increase in the L/D ratio initially reduces the overall drag, and then after L/D = 1.5, the overall drag is reduced. Since the further in the L/D after increases the skin friction drag, overall drag increases. The helmet has an L/D ratio of 1.5, offers the least drag, and is selected for further experimentation. The helmet with an L/D ratio of 1.5 is manufactured using 3D printing and used in the wind tunnel investigation.

3. Manufacturing and experimentation

3.1 Manufacturing

The helmet models with a boat tail and without boat-tail are manufactured using 3D printing.

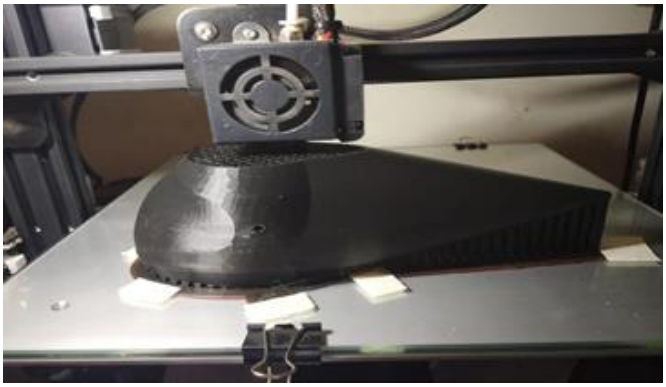

Fig. 6 Manufacturing of helmet using 3D printing technology

Fig. 7 A manufactured helmet without boat tail

Fig. 8 Manufactured helmet with a boat tail

The L/D ratio of boat-tailed helmets considered for manufacturing was 1.5. All the dimensions of the helmet were reduced for manufacturing with a constant scale factor. Fig. 6 shows the process of manufacturing the boat-tail helmet with 3D printing. Figs. 7 and 8 show the helmet's shape without boat tail and with boat-tail. The scaled manufactured helmet's overall dimensions without boat-tail are; Length = 96 mm, Width = 75 mm, and height = 76 mm. The scaled

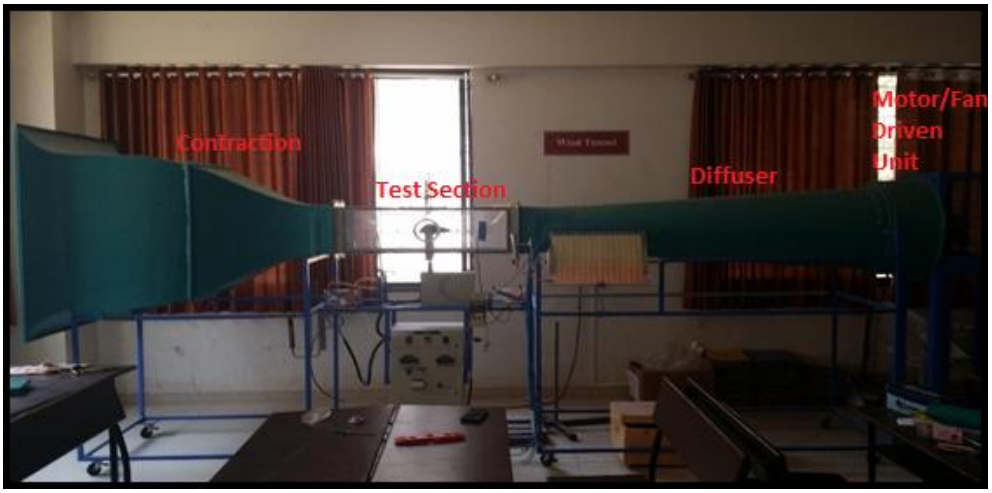

Fig. 9 Experimental setup of wind tunnel

manufactured helmet's overall dimensions with boat-tail are; Length = 200 mm, Width = 75 mm, and height = 76 mm.

3.2 Experimentation

This section describes the wind tunnel experiment's details at the wind tunnel facility located at Trinity College of Engineering and Research, Pune. Fig. 9 demonstrates the wind tunnel facility and the different components used inside the wind tunnel. The wind tunnel had played a leading role in aerodynamic performance analysis since the first days of powered flight when the Wright Brothers used a wind tunnel to evaluate the lift and drag of their airfoil profiles. Mounting the model on a force balance allows the measurement of forces such as drag and lift as the air interacts with the scale model.

4. Results

Wind tunnel experimentation results in the original helmet without the cone and with the cone at different velocities. The experiments were performed for both the models of the helmet as velocities 5, 10, 15, 20, 25, 30 m/s. The CFD analysis was carried out for the helmet models with a reduced dimension as used in the experimentation for velocity up to 70 m/s. The experimental and CFD results of the drag coefficient (Cd) are shown in Fig. 10.

From Fig. 10, it is seen that there is a considerable reduction in the overall drag on the helmet with a modification in the shape of the helmet in terms of boat-tail. The effectiveness of the improvement on the drag increases with an increase in the velocity. The CFD and experimental results show excellent agreement with negligible error.

Figs. 11 and 12 show the contour plots for drag vs. boat tail and velocity based on experimental results and CFD results, respectively. From Figs. 11 and 12 shows that the drag is reduced with the modification in the helmet's shape. When the boat tail is attached to the helmet, the drag is reduced at all velocities' values. The vertical axis boat tail stands for the presence of boat tail, i.e., '1' stands for with boat-tailed model and '0' stands for without boat-tailed model.

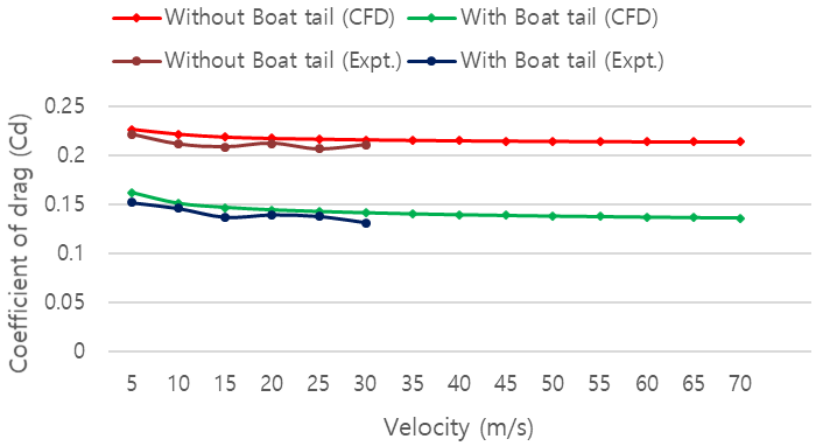

Fig. 10 Drag coefficient (Cd) of helmet models at various velocities

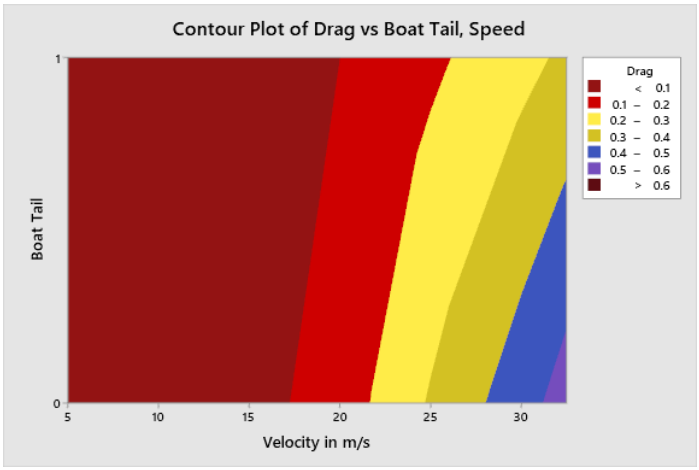

Fig. 11 Contour plot for overall drag based on experimental results

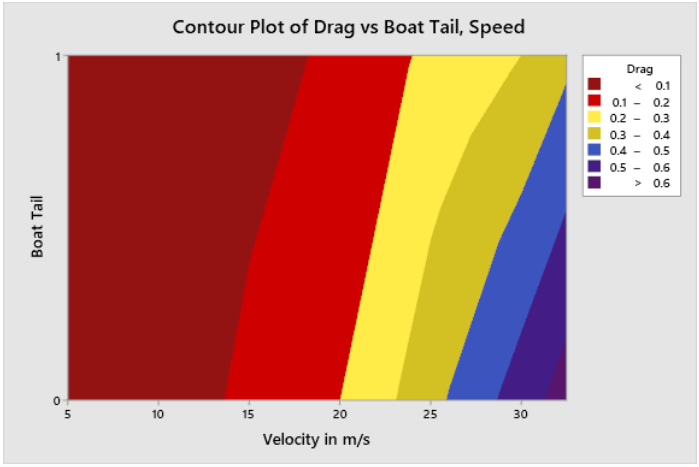

Fig. 12 Contour plot for overall drag based on CFD results

5. Conclusions

Based on this research work using CFD analysis and experimentations, the following important point concerning aerodynamic drag acting on the helmet body is concluded. The aerodynamic drag increases with the increase in velocity; a massive difference between aerodynamic drag is seen at high velocities. The aerodynamic drag reduces when the shape of the helmet is streamlined. The aerodynamic drag is further reduced by introducing a streamlined body, i.e., boat tail at the helmet's rear end. The boat tail helmet offers minimum drag at an L/D ratio of 1.5. With a further increase in the L/D ratio, the drag increases due to the skin friction effect. By introducing the boat tail at the rear end of the helmet, there is a maximum reduction in drag compared with the basic helmet in the wind tunnel experimentation and CFD analysis. The coefficient of drag achieved by introducing boat tail is 0.14.

Acknowledgments

All the authors would like to thank the management of Trinity College of Engineering and Research, Pune, India, for providing a wind tunnel facility for the experimentation.

References

Aabid, A., Khairulaman, L.N.B. and Khan, S.A. (2021), "Analysis of flows and prediction of CH10 airfoil for unmanned arial vehicle wing design", *Adv. Aircraft Spacecraft Sci.*, **8**(2), 87-109. https://doi.org/10.12989/aas.2021.8.2.087.

Alam, F., Chowdhury, H., Wei, H. Z., Mustary, I. and Zimmer, G. (2014), "Aerodynamics of ribbed bicycle racing helmets", *Procedia Eng.*, **72**, 691-696. https://doi.org/10.1016/j.proeng.2014.06.117.

Beaumont, F., Taiar, R., Polidori, G., Trenchard, H. and Grappe, F. (2018), "Aerodynamic study of time-trial helmets in cycling racing using CFD analysis", *J. Biomech.*, **67**, 1-8. https://doi.org/10.1016/j.jbiomech.2017.10.042.

Brownlie, L., Ostafichuk, P., Tews, E., Muller, H., Briggs, E. and Franks, K. (2010), "The wind-averaged aerodynamic drag of competitive time trial cycling helmets", *Procedia Eng.*, **2**(2), 2419-2424. https://doi.org/10.1016/j.proeng.2010.04.009.

Kalimuthu, R., Mehta, R.C. and Rathakrishnan, E. (2019), "Measured aerodynamic coefficients of without and with spiked blunt body at Mach 6", *Adv. Aircraft Spacecraft Sci.*, **6**(3), 225-238. http://doi.org/10.12989/aas.2019.6.3.225.

Khan, S.A., Fatepurwala, M.A. and Pathan, K.N. (2019a), "CFD analysis of human powered submarine to minimize drag", *Int. J. Mech. Prod. Eng. Res. Develop.*, **8**(3) 1057-1066. https://doi.org/10.24247/ijmperdjun2018111.

Mannion, P., Toparlar, Y., Blocken, B., Clifford, E., Andrianne, T. and Hajdukiewicz, M. (2018), "Aerodynamic drag in competitive tandem para-cycling: Road race versus time-trial positions", *J. Wind Eng. Ind. Aerod.*, **179**, 92-101. https://doi.org/10.1016/j.jweia.2018.05.011.

Mehta (2020), "Drag reduction for payload fairing of satellite launch vehicle with aerospike in transonic and low supersonic speeds", *Adv. Aircraft Spacecraft Sci.*, **7**(4), 371-385. https://doi.org/10.12989/aas.2020.7.4.371.

Meng, Y.S., Yan, L., Huang, W., Ji, C. and Li, J. (2021), "Coupled investigation on drag reduction and thermal protection mechanism of a double-cone missile by the combined spike and multi-jet", *Aerosp. Sci. Technol.* **115**, 1-17. https://doi.org/10.1016/j.ast.2021.106840.

Pathan, K.A., Ashfaq, S., Dabeer, P.S. and Khan, S.A. (2019), "Analysis of parameters affecting thrust and

base pressure in suddenly expanded flow from nozzle", *J. Adv. Res. Fluid Mech. Thermal Sci.*, **64**(1), 1-18.

Pathan, K.A., Dabeer, P.S. and Khan, S.A. (2020), "Enlarge duct length optimization for suddenly expanded flows", *Adv. Aircraft Spacecraft Sci.*, **7**(3), 203-214. https://doi.org/10.12989/aas.2020.7.3.203.

Quadros, J. D., Khan, S. A., Sapkota, S. and Vikram, J. (2020), "On recirculation region length of suddenly expanded supersonic flows, using CFD and fuzzy logic", *Int. J. Comput. Fluid D.*, **34**(6), 1-17. https://doi.org/10.1080/10618562.2020.1828580.

Sathish Gandhi, V.C., Kumaravelan, R., Ramesh, S., Venkatesan, M. and Siva Rama Krishnan, M. (2014), "Aerodynamic design and analysis of motorcycle helmet with anti-glare visor", *Tehnički glasnik*, **8**(1), 97-101.

Shaikh, S.K., Pathan, K.A., Chaudhary, Z.I. and Khan, S.A (2020), "CFD analysis of an automobile catalytic converter to obtain flow uniformity and to minimize pressure drop across the monolith", *CFD Lett.*, **12**(9), 116-128. https://doi.org/10.37934/cfdl.12.9.116128.

EC